PAPER • **OPEN ACCESS**

Process parameters optimization for producing AA6061/(Al_2O_3, Gr and Al_2O_3+Gr) surface composites by friction stir processing

To cite this article: B R EL-Eraki *et al* 2019 *IOP Conf. Ser.: Mater. Sci. Eng.* **610** 012006

IOP Conf. Series: Materials Science and Engineering **610** (2019) 012006 doi:10.1088/1757-899X/610/1/012006

Process parameters optimization for producing AA6061/ (Al_2O_3, Gr and Al_2O_3+Gr) surface composites by friction stir processing

B R EL-Eraki[1,3], A R EL-Sissi[1], S M Khafagi[2] and H S Nada[1]

[1]Production Engineering and Mechanical Design Department, Faculty of Engineering, Menoufia University, Shebin El-kom, Menoufia, Egypt
[2]Tabbin Institute for Metallurgical Studies, Egypt

[3]Email: eng.basma812@yahoo.com

Abstract. The present study uses Al_2O_3, graphite and hybrid Al_2O_3 and graphite nanoparticles as reinforcement particles within AA 6061 to produce a surface composite metal matrix using multiple-pass FSP. The aim of this work is to investigate the effects of multi-pass FSP, type of reinforcement particles and effects of T6 post-treatments on the microstructure and mechanical properties (hardness, ultimate tensile strength, and elongation) of friction stir processed (FSPed) AA6061 alloy. The results show that; all the composites produced using alumina particles in matrix material have the highest ultimate tensile strength (213 Mpa). Increase in hardness of stir zone for FSPed samples was more pronounced with post heat treatment and essentially insignificant for variation in a number of passes. The process parameters were optimized using a Taguchi method. The most influential parameter was a type of reinforcement particles. The analysis of variance (ANOVA) used to evaluate the percentage contribution for each parameter.

1. Introduction

Aluminium and its alloys are usually utilized in much modern industrial application such as aerospace, automotive, and shipbuilding industries, this attributed to its good strength to weight ratio, better corrosion resistance, and high electrical and thermal conductivity however they exhibit poor tribological properties [1]. AA6061 is an exact alloy of 6xxx series and includes some alloying elements such as Al-Mg-Si [2]. Aluminium metal matrix composites (AMMCs) are usually replacing conventional aluminium alloys in several applications due to higher mechanical properties and tribological properties. Those attributed to the presence of nano and micro-sized reinforcement particles (RP) in the matrix. Wide researches carried out to improve the properties of AMCs using different fabrication methods and reinforcements can be the ceramic particles, whiskers, flakes, and fibres of various types. The commonly used reinforcements include SiC, Gr, TiC, Al_2O_3, AlN, MoS_2, B_4C, TiB_2, TiO_2, etc., or a mixture of them and others are commonly used as reinforcement in the composites [3]. The applications of Al_2O_3 particle reinforced aluminium alloy matrix composites in the automotive and aircraft extended. However, "the use of graphite reinforcement in a metal matrix improved wear and lubrication properties of the materials, whereas at higher graphite addition levels a complete reversal in the wear behaviour

was observed" [4]. Due to its wide application, graphite (Gr) and alumina (Al_2O_3) used as reinforcements in present work. In addition, Al/Al_2O_3/Gr hybrid nano composites find wide application in advanced engineered materials due to their tribological applications. The scope of Al/Al_2O_3/Gr nano-composites has great interest in tribological applications in automotive and aerospace industries. "The usage of hybrid Al/Al_2O_3/Gr self-lubricating nano composite components leads to reduce the oil consumption, power loss and maintenance cost"[5].

Friction stir processing (FSP)," is a recent technology that is based on the principles of friction stir welding (FSW) developed at the welding institute (TWI) of UK in 1991 for aluminium alloys" [6]. FSP is a solid-state processing technique used for surface modification and developing surface and MMCs, which improves the mechanical properties and microstructure. Farther, FSP produced severe plastic deformation to MMCs in stir zone (SZ), which leads to ultra-refinement and homogeneous distribution of particles in the AMCs depending on the process parameters employed. The welding in FSP occurred in double pass (rather than single pass as an FSW) one forward, and the other to return along the joint line to achieve maximum performance with low production cost in less time as illustrated in Figure.1(a - b) [7]. The process considered as a green technology, as it does not produce any fumes and harmful gases and noise like in other conventional techniques. The temperatures developed during the FSP was below the melting point of the material to be processed, which avoids interfacial reactions and avoids defects like pinhole porosity and air inclusions.

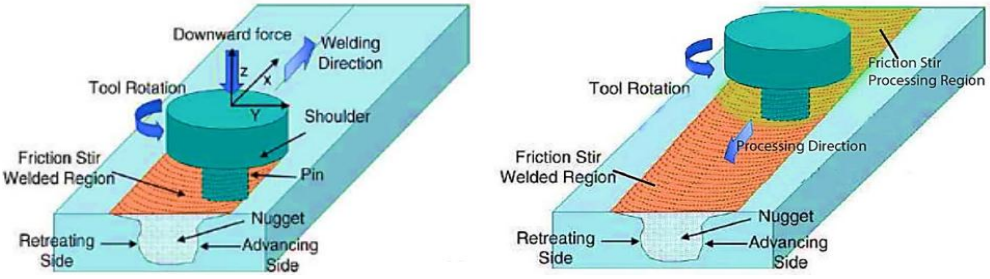

(a) (b)

Figure 1. Schematic diagram of (a) FSW/ and (b) FSP joints [7].

Extensive researches carried out in MMCs and surface composites of aluminium alloys via FSP [8-11]. In the case of a surface composite process, multi-pass FSP considered an effective method to improve the distribution and dispersion of the reinforcement particles in the composite matrix [12-16].

The properties of some AMMCs can significantly be improved via heat treatment, especially 2xxx and 6xxx series alloys [17]. Previous studies show that the microstructure and mechanical properties of FSP Al alloys, and their composites improved via several treatments after or during the welding[18, 19].

Optimization of FSP parameters used to reduce the number of experiments, time, and cost. Taguchi method and the analysis of variance (ANOVA) used to study the effect of process parameters on the FSP. Wide researches carried out in metal matrix composites and surface composites of aluminium alloys using FSP optimization[20].

The aims of the present research are. (a) fabrication of AA6061/ (Al_2O_3, Gr, and hybrid Al_2O_3+Gr) surface composites via FSP (b) investigate the effects of type of reinforcement (alumina, graphite, and alumina with graphite) on the microstructure, hardness distribution and tensile properties of friction stir processed (FSPed) AA6061 alloy. (c) Effects of T6 post heat treatment treatments (PHT) on the mechanical properties and microstructure characteristics of the FSP joints. (d) The effect of a number of passes on the mechanical properties and microstructure characteristics of the FSP joints. (e) Process parameters optimization using Taguchi analysis of the above-mentioned input parameters, and ANOVA to know the percentage contribution of each parameter.

2. Experimentation

2.1. Experimental procedure

In this study, the parameters and levels designated and produced L18 matrix using MINITAB18 software as listed in table 3 and table 4. Taguchi method used to optimize processing parameters for responses of hardness, UTS, and percentage of elongation. The percentage contribution of process parameters expected using Analysis of Variance (ANOVA).

The AA 6061sheet alloy with dimensions of (100*50*4) mm has a chemical composition and mechanical properties given in Table 1 and Table 2 respectively. Nano particles of graphite (with an average diameter 100 nm), Al_2O_3 (with an average diameter 50 nm) have been used to reinforce aluminium metal matrix nano composites (AMMNCs) via FSP. The base metal sheets were prepared and machined for a suitable size. The plates were grooved with 0.8 mm width and 3 mm depth FSP. An automatic vertical milling machine used for processing, as shown in Figure. 1(a). HSS tool used as a tool for FSP. The tool without pin was fitted to compact the powder into a squared groove to prevent the powder from escaping out and other tool with a threaded cylindrical pin are used to make an FSP. Figure. 2 (a - b) shows FSP tool used in the process. The tool was machined to obtain thread cylindrical shape with a shoulder diameter of (Ø25 mm), a pin diameter of (Ø4.5 mm) and tool pin has a 3 mm length. Tool rotation speed 1060 rpm and travel speed of 42 mm/min chosen after a number of trials. With tool, tilt angle of 2 degrees. One, two and three passes performed in the processing. Figure. 3 Shows typical AMMNC after FSP.

Table 1. Chemical composition of 6061 aluminum alloy (wt. %)

Alloy	Mg	Si	Fe	Cu	Cr	Mn	Zn	Ti	Al
6061	0.9	0.62	0.33	0.28	0.17	0.06	0.02	0.02	Balance

Table 2. Mechanical properties of 6061 aluminum alloy.

Alloy	S_Y (Mpa)	UTS (Mpa)	Elongation %	Hardness(HR)
6061	110	207	16	40

Table 3. Process parameters and their levels

Levels → Process parameters↓	1	2	3
Post-treatment	(T6)	Without (T6)	
Type of reinforcement	Al_2O_3	Gr	Al_2O_3 + Gr
No. of passes	1	2	3

After FSP, the cutting and preparation of samples performed to produce microstructural, tensile strength, hardness examinations. The micro structural observations performed at a cross section of SZ normal to the FSP direction. The samples are polished and etched with Keller's Agent (2 ml HF (2%) + 98 ml distilled water) at room temperature for a few seconds until the desired contrast achieved. The microstructures performed via an optical microscope (model Leco LX 31-USA). The tensile specimens were prepared as per the ASTM E-8 standards to the required dimensions as shown in Figure. 4. The tensile test conducted on the computer controlled universal testing machine (model WDW-300). Hardness was measured in SZ using a hardness tester (INNOVA TEST) with a dwell time of 5 sec at SZ.

Table 4. Taguchi matrix (L18)

Exp. No.	Treatment	Type of reinforcement	No. of passes
1	T6	Al_2O_3	1
2	T6	Al_2O_3	2
3	T6	Al_2O_3	3
4	T6	Gr	1
5	T6	Gr	2
6	T6	Gr	3
7	T6	Al_2O_3 + Gr	1
8	T6	Al_2O_3 + Gr	2
9	T6	Al_2O_3 + Gr	3
10	Without T6	Al_2O_3	1
11	Without T6	Al_2O_3	2
12	Without T6	Al_2O_3	3
13	Without T6	Gr	1
14	Without T6	Gr	2
15	Without T6	Gr	3
16	Without T6	Al_2O_3 + Gr	1
17	Without T6	Al_2O_3 + Gr	2
18	Without T6	Al_2O_3 + Gr	3

2.2. Thermal treatments

The thermal treatments consist of two steps. The first is a solution treatment and the second one is the aging treatment. The solution treatment performed to dissolve all the precipitates present in the material to make the alloying elements available for subsequent controlled precipitation during aging. The treatments made at 520°C for 45 min as suggested in the literature [21-23] in a heat treatment electrical furnace with a power of 12kW. The samples quenched in water to obtain a final higher hardness. In fact, the fast cooling avoids the precipitation of intermetallic compounds during this stage, ensuring a better result of the aging. After the solution, the samples lifted for a week -5°C. The aging treatment was carried out at 175°C for 8 hours and performed in dryer (1.1 kW) furnace.

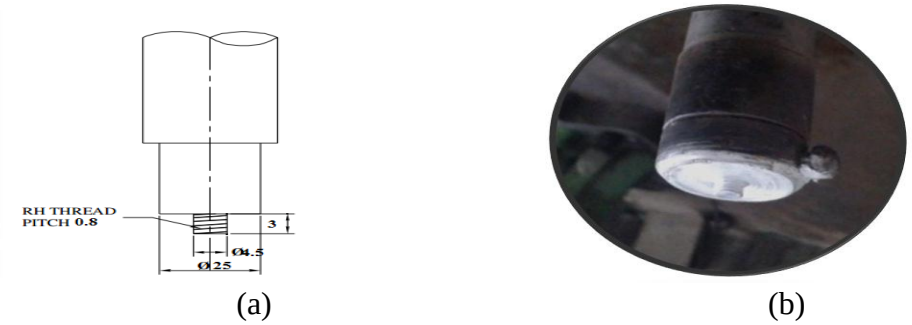

Figure 2. (a) Dimension of the tool used in FSP (b) Typical tool used in process.

Figure. 3 AMMNC after FSP

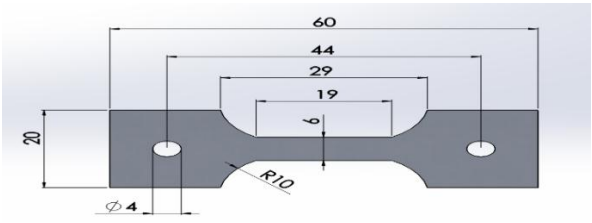

Figure 4. Standard dimension of tensile specimen.

3. Results and discussion

3.1. Microstructure

Figure. 5(a - b) shows typical micrographs of the microstructure of the AA6061 Al alloy base metal (BM) before and after T6 heat treatment respectively. In both, the microstructure of BM consists of rough elongated α-Al primary grains with coarse Mg_2Si particles due to rolling at which the plate has been subjected. Meanwhile, T6 treatment dissolves most of the Mg_2Si particles within the matrix.

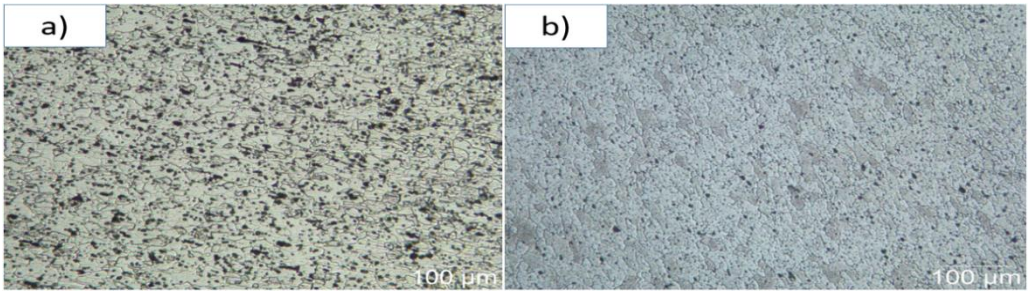

Figure 5. Microstructure of base metal (a) AA 6061 (b) AA 6061 after T6 heat treatment

Figure s. 6-9 shows typical optical micrographs of the stir zones of samples produced with and without powder. The size of the SZ is generally about equal to the size of the pin, width, and depth of 4.5 mm and 3 mm, respectively. It is very clear that the microstructure of the FSP regions differs that of the base alloy. The FSP zones exhibited a much more homogenous microstructure as compared to the base alloys. Figure. 6(a-c) shows microstructure of stir zones in composite samples produced via one to three passes respectively. Base metal AA6061 structure destroyed and precipitates were uniform homogeneously distributed throughout the SZ. The stirring action of the FSP tool resulted in the fragmentation of Mg_2Si particles, there by caused more refinement. Within the SZ, a fine grain structure observed; due to the

dynamic recrystallization (DR) caused via severe plastic deformation (SPD) and increase in temperature. Earlier researchers found that microstructural modifications were observed due to FSP [24-26] and the similar observations were observed in this investigation. As reported via other researchers, SPD and heat input produce fine grains via DR McNelley, et al. [27]. Therefore, the grain size of the SZ decreased with an increase in the number of FSP pass, which is due to a larger strain extruded via higher passes. However, the multiple pass FSP with the nano-sized particles more effectively reduced the grain size of the 6061Al matrix as shown in Figure. 6(a-c).

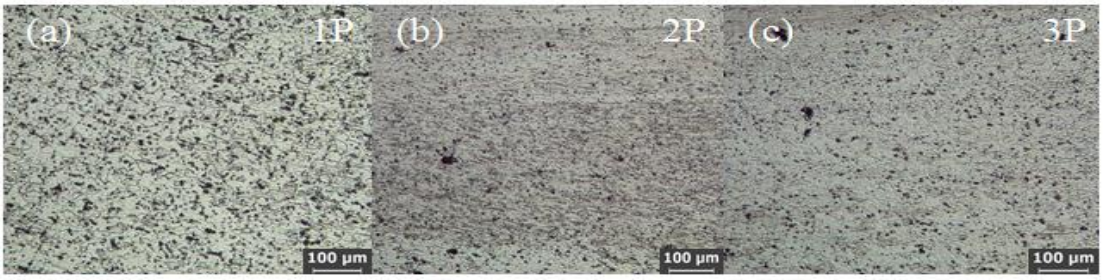

Figure 6. Stir zone microstructures of samples produced via FSP and without powder at condition (1060 rpm and 42 mm/min) and after (a) 1st Pass (b) 2nd Pass (c) 3rd Pass.

In AA6061/ Al_2O_3 nano surface composite, according to the nature of metal flow in the stirring zone during FSP, nonhomogeneous dispersion and agglomeration of Al_2O_3 nanoparticles formed at the SZ for specimens produced at first and second passes with the change direction of rotational speed of FSP as shown in Figures. 7(a, b). This is because of the limited amount of metal flow and low plasticity at first and second passes. Further, clustering of particles is attributed to less amount of heat generation between tool shoulder and the sheet metal, which is insufficient to cause a considerable amount of metal flow around the pin. During the third pass of FSP, the accumulated clusters of Al_2O_3 nanoparticles were refined and well distributed at the stirring zone as shown in Figure. 7 (c).

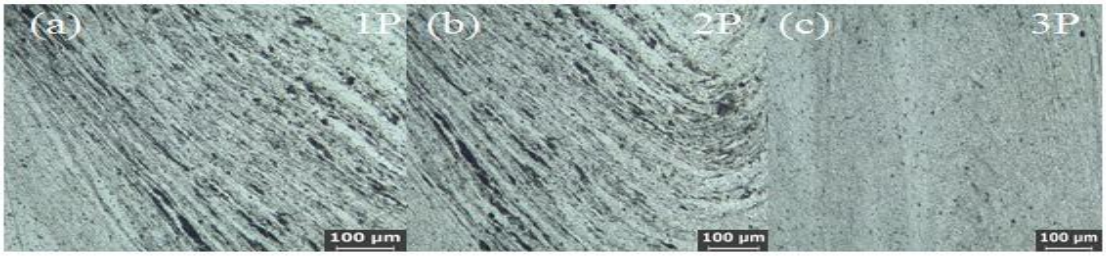

Figure 7. Stir zone microstructures of samples produced via FSP of AA6061/ Al_2O_3 at condition (1060 rpm and 42 mm/min) and after (a) 1st Pass (b) 2nd Pass (c) 3rd Pass.

With AA 6061/Gr nano surface composite, Figure. 8 shows the effect of pass a number on the distribution of graphite nanoparticles during FSP. It was evidenced that, the almost uniform and homogeneous distribution of graphite particles over the matrix surface occurred at third pass more than the first and second pass. Graphite reinforcement procedures a rich film of lubricant during FSP which helps in the decrease of shear stress to be transferred to the matrix and thus increases the plastic deformation just below the surface These results are in similar with the previous researches done via Prakash, et al. [28]. This continuous solid graphite film uniformly distributed as appeared in Figure. 10(h, j).

Figure 8. Microstructures of SZ for samples produced via FSP of AA 6061/ Gr at condition (1060 rpm and 42 mm/min) and after Al_2O_3 after (a) 1st Pass (b) 2nd Pass (c) 3rd Pass.

With hybrid AA 6061/Gr/ Al_2O_3 nano surface composite and due to high thermal conductivity of graphite, the softening effect counteracted via the existence of hard Al_2O_3 abrasive particles. Figure. 9(a-c) reveals the OM images of AA 6061strengthened with hybrid graphite and Al_2O_3 processed at multi-pass FSP. It was observed that, non-homogenous dispersion of Al_2O_3 particles take place, however, the graphite particles are uniformly distributed. Figure. 10 shows typical microstructures of all samples produced via FSP after heat treatment (T6). It was observed that, Post weld solution treatment produces a super wet solid solution throughout the weld and the following aging treatment led to homogeneous re-precipitation leading higher hardness.

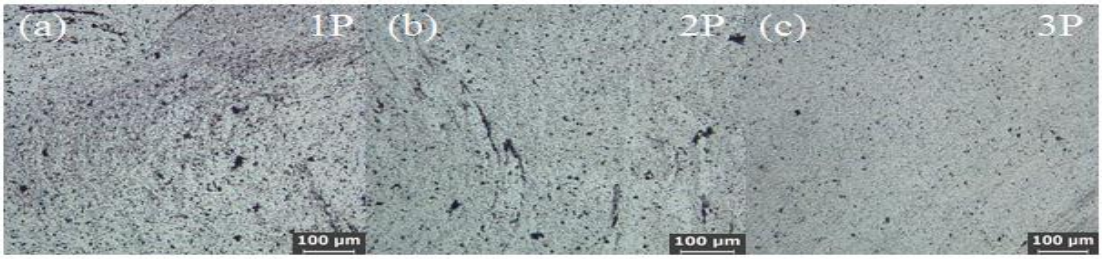

Figure 9. Microstructures of samples produced via FSP of AA6061/ Al_2O_3 /Gr at condition (1060 rpm and 42 mm/min) and after (a) 1st Pass (b) 2nd Pass (c) 3rd Pass.

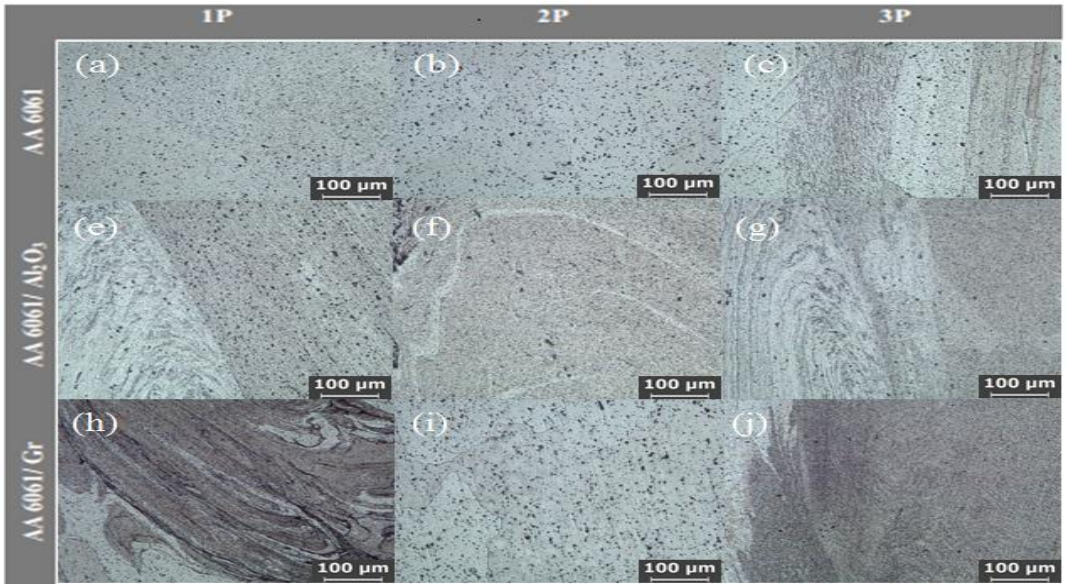

Figure 10. Microstructures of samples produced via FSP at condition (1060 rpm and 42 mm/min) and after heat treatment (T6).

3.2. Mechanical properties

The Rockwell's hardness tests were conducted on the static tests specimens, at intervals of 5 mm along the mid-plane of the sheets. The values of a hardness of specimens at SZ listed in table 5. From the results, it was observed that all samples that exposures to post heat treatment have a significant increase in hardness. This could be attributed to the fine precipitates formed after artificial aging (T6) as well as the grain refining effect. Throughout solution treatment, produced a dissolution of the precipitates in the matrix and form super saturated solid solution upon cooling. These results are in similar to the previous researches done via [19, 29]. In addition, due to the nature of Al_2O_3 particles as hardness phase, the FSPed samples of AA6061/ (Al_2O_3 and hybrid Al_2O_3 + Gr) that have a significant increase in the hardness. Moreover, an increasing a number of passes almost produced uniform distribution or homogeneous distribution of Al_2O_3 and Gr particles over the matrix surface especially for the third pass and hence, it exhibited a higher value of hardness.

Ultimate tensile strength (UTS) and percentage of elongations were evaluated and listed in Table 5. It was observed that, UTS of FSPed composite reduced than as-received AA6061 due to weak bonding and loss of precipitates of reinforcement to the matrix. These results are in similar with the previous research done via Aruri, et al. [30] Aruri, et al. [30]. In addition, all FSPed samples produced using alumina as reinforcement particles in matrix material before and after heat treatment have high ultimate tensile strength (213 Mpa). And also, that all the samples produced at three passes have high ultimate tensile strength. All samples fractured in the NZ and TMAZ. Farther more, due to using graphite as a solid lubricant, all samples produced via FSPed using graphite as reinforcement have lower values of elongation as shown in Figure.12.

4. Process optimization

4.1. Optimization using Taguchi method.

Taguchi's method is applied for response optimization. Hardness, Ultimate tensile strength (UTS) and Elongation percentage were examined to optimize the processing parameters. The larger the better condition selected for all responses to maximize responses. The mean S/N ratio for two and three levels of process parameters was presented in table 6, table 7 and table 8. Based on the mean response tables of S/N ratio, optimal parameters for each parameter were identified with a larger value of S/N ratio. The optimal parameters for hardness are type of reinforcement particles of hybrid (Al_2O_3 + Gr), post-treatment (T6) and a number of passes (3). However for UTS, type of reinforcement particles of Al_2O_3, post-treatment (without treatment) and a number of passes (3). For the percentage of elongation are a type of reinforcement particles of Al_2O_3, post-treatment (without treatment), and a number of passes (3). From response tables, type of particles ranks first in the contribution of UTS and percentage of elongation next followed via of a number of passes and post-treatment (T6). Reinforcement ranks first and followed post-treatment (T6), and a number of passes for hardness. Figure.s 11-13 show main effects plot for S/N ratios for hardness, UTS and percentage of elongation responces respectively.

4.2. Analysis of variance (ANOVA)

The aim of the ANOVA used to identify the most significant parameter on the output responses and study the effect of each input parameters on the responses. "Usually, the change of the process parameter has a significant effect on the responses, when P value is smaller and F is larger"[3]. The results of the ANOVA were presented in Table 9. The type of reinforcement has 41.3% contribution in the output response for Hardness followed via post-treatment (T6) and a number of passes. The type of reinforcement has 43.44% contribution in the output response for UTS followed via a number of passes and post-treatment (T6). The type of reinforcement has 45.3% contribution in the output response for UTS then a number of passes and post-treatment (T6).

Table 5. Output characteristic and S/N ratio

Exp. No.	Hardness (RHf)	UTS (MPa)	Elongation%	S/N for Hardness	S/N for UTS	S/N for E %
1	68.60	189.240	11.60	36.7265	45.5403	21.2892
2	61.70	167.500	2.40	35.8057	44.4803	7.6042
3	66.10	213.200	15.10	36.4040	46.5757	23.5795
4	64.50	100.460	2.90	36.1912	40.0399	9.2480
5	63.10	88.030	2.70	36.0006	38.8926	8.6273
6	65.70	175.000	12.90	36.3513	44.8608	22.2118
7	67.60	150.000	6.80	36.5989	43.5218	16.6502
8	63.70	151.000	8.95	36.0828	43.5795	19.0365
9	67.20	111.440	12.11	36.5474	40.9408	21.6629
10	66.00	200.000	20.70	36.3909	46.0206	26.3194
11	62.64	199.075	21.60	35.9370	45.9803	26.6891
12	69.72	199.588	22.20	36.8671	46.0027	26.9271
13	46.00	191.320	4.20	33.2552	45.6352	12.4650
14	43.30	190.923	4.00	32.7298	45.6172	12.0412
15	54.33	205.900	6.60	34.7008	46.2731	16.3909
16	67.60	91.950	4.40	36.5989	39.2710	12.8691
17	63.70	105.725	6.50	36.0828	40.4836	16.2583
18	67.20	153.000	8.60	36.5474	43.6938	18.6900

Table 6. Signal to noise ratios for hardness larger is better

Levels → Process parameters↓	Post-treatment	Type of reinforcement	No. of passes
1	**36.30**	36.36	35.96
2	35.46	34.87	35.44
3		**36.41**	**36.24**
Delta	0.84	1.54	0.80
Rank	2	1	3

Table 7. Signal to noise ratios for UTS larger is better

Levels → Process parameters↓	Post-treatment	Type of reinforcement	No. of passes
1	43.16	**45.77**	43.34
2	**44.33**	43.55	43.17
3		41.92	**44.72**
Delta	1.17	3.85	1.55
Rank	3	1	2

Table 8. Signal to noise ratios for percentage of elongation larger is better.

Levels → Process parameters↓	Post-treatment	Type of reinforcement	No. of passes
1	16.66	**22.07**	16.47
2	**18.74**	13.50	15.04
3		17.53	**21.58**
Delta	2.08	8.57	6.53
Rank	3	1	2

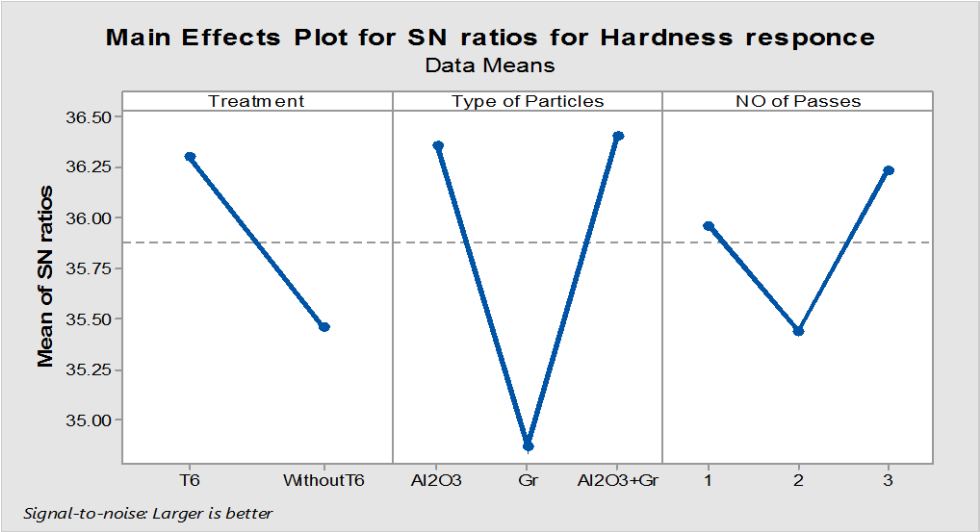

Figure 11. Main effects plot for S/N ratios for hardness responce.

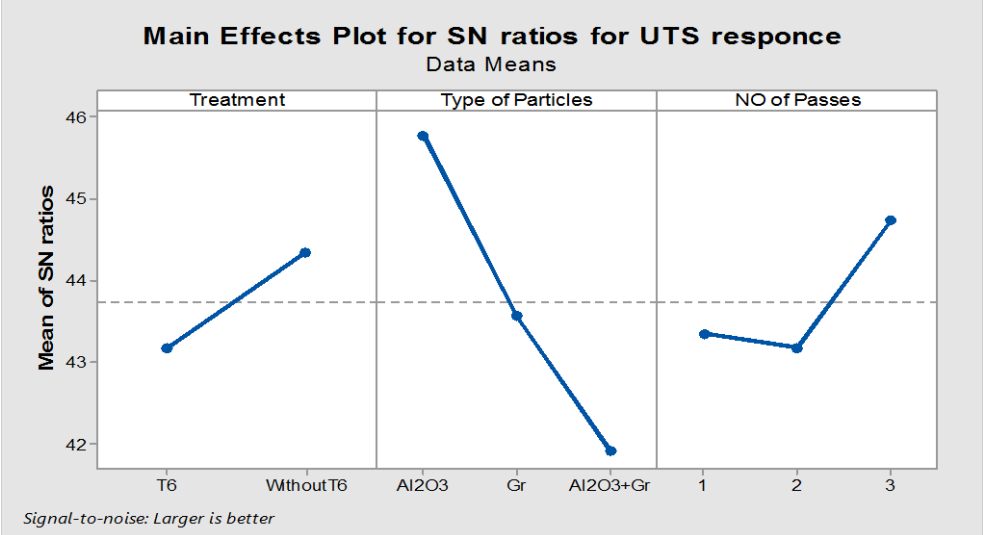

Figure 12. Main effects plot for S/N ratios for UTS responce.

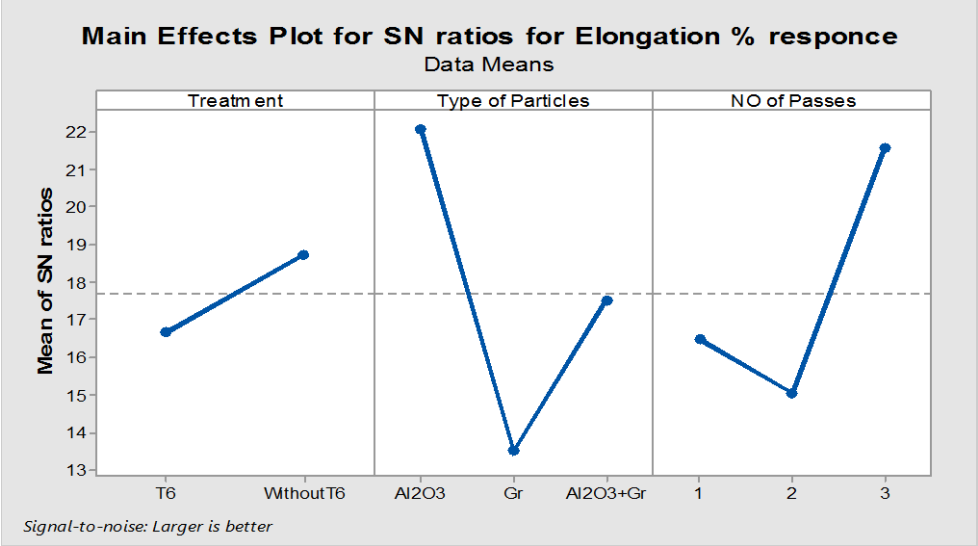

Figure 13. Main effects plot for S/N ratios for pecentage of elongation responce.

Table 9. Analysis of variance (ANOVA)

Process parameter	DF	Adj SS	Adj MS	F-Value	P-Value
A) For Hardness					
Treatment	1	126.46	126.46	4.56	0.054
Type of Particles	2	386.54	193.27	6.97	0.010
NO. of Passes	2	90.06	45.03	1.62	0.238
Error	12	332.71	27.73		
Total	17	935.77			
B) for UTS					
Treatment	1	2040	2040	1.82	0.202
Type of Particles	2	13724	6862	6.13	0.015
NO. of Passes	2	2389	1194	1.07	0.375
Error	12	13441	1120		
Total	17	31593			
C) for E%					
Treatment	1	30.26	30.26	1.30	0.276
Type of Particles	2	331.77	165.89	7.13	0.009
NO. of Passes	2	95.97	47.98	2.06	0.170
Error	12	279.06	23.26		
Total	17	737.06			

5. Conclusions

The AA 6061/ (Al_2O_3, Gr, and Al_2O_3+Gr) surface composites successfully fabricated via friction stir processing. The microstructure observations showed a homogeneous distribution of particles for the third pass in all composites. Nano-scale of Al_2O_3 particles seems to be more efficient in increasing hardness and UTS. Hardness increase of SZ for FSPed samples was more pronounced with post heat treatment (T6) and with the third pass. The ANOVA results indicated that the type of particles found to be the most influential process parameter for Hardness and UTS with 41.30 % and 44.43% respectively. The analysis definite that, multi-pass FSP without a change in direction of rotational speed not only achieves a refinement in the grain size but also displays a homogeneous distribution of the reinforcement particles.

6. References

[1] H. Bakes, D. Benjamin, and C. W. K. (Eds.), "Metals Handbook," vol. 2, pp. 3-23, 1979.
[2] Z. Nikseresht, F. Karimzadeh, M. Golozar, and M. Heidarbeigy, "Effect of heat treatment on microstructure and corrosion behavior of Al6061 alloy weldment," Materials & Design (1980-2015), vol. 31, pp. 2643-2648, 2010.
[3] D. R. Santha and N. Ramanaiah, "Process Parameters Optimization for Producing AA6061/TiB2 Composites by Friction Stir Processing," Strojnícky casopis–Journal of Mechanical Engineering, vol. 67, pp. 101-118, 2017.
[4] A. Zeren, "Effect of the graphite content on the tribological properties of hybrid Al/SiC/Gr composites processed by powder metallurgy," Industrial Lubrication and Tribology, vol. 67, pp. 197-201, 2015.
[5] I. Manivannan, S. Ranganathan, S. Gopalakannan, and S. Suresh, "Dry Sliding Wear behaviour of cast Al/Al_20_3/Gr hybrid nano-composite using response surface methodology," in IOP Conference Series: Materials Science and Engineering, 2018, p. 012105.
[6] R. S. Mishra and Z. Ma, "Friction stir welding and processing," Materials science and engineering: R: reports, vol. 50, pp. 1-78, 2005.
[7] M. A. Al-Shammari and W. H. Ibrahim, "Effect of Friction Stir Welding and Friction Stir Processing Parameters on The Efficiency of Joints," Al-Nahrain Journal for Engineering Sciences, vol. 21, pp. 230-237, 2018.
[8] R. S. Mishra, Z. Ma, and I. Charit, "Friction stir processing: a novel technique for fabrication of surface composite," Materials Science and Engineering: A, vol. 341, pp. 307-310, 2003.
[9] P. Cavaliere, E. Cerri, L. Marzoli, and J. Dos Santos, "Friction stir welding of ceramic particle reinforced aluminium based metal matrix composites," Applied Composite Materials, vol. 11, pp. 247-258, 2004.
[10] Y. X. Gan, D. Solomon, and M. Reinbolt, "Friction Stir Processing of Particle Reinforced Composite Materials," Materials, vol. 3, pp. 329-350, 2010.
[11] H. Arora, H. Singh, and B. Dhindaw, "Composite fabrication using friction stir processing—a review," The International Journal of Advanced Manufacturing Technology, vol. 61, pp. 1043-1055, 2012.
[12] E. Moustafa, "Effect of Multi-Pass Friction Stir Processing on Mechanical Properties for AA2024/Al_2O_3 Nanocomposites," Materials, vol. 10, p. 1053, 2017.
[13] M. M. El-Rayes and E. A. El-Danaf, "The influence of multi-pass friction stir processing on the microstructural and mechanical properties of Aluminum Alloy 6082," Journal of Materials Processing Technology, vol. 212, pp. 1157-1168, 2012.
[14] A. Rao, V. Katkar, G. Gunasekaran, V. Deshmukh, N. Prabhu, and B. Kashyap, "Effect of multipass friction stir processing on corrosion resistance of hypereutectic Al–30Si alloy," Corrosion Science, vol. 83, pp. 198-208, 2014.
[15] C. D. Singh, R. Singh, and N. Kumar, "Effect of FSP Multipass on Microstructure and Impact Strength of AL6063," American International Journal of Research in Science, Technology, Engineering & Mathematics, vol. 6, pp. 140-145, 2014.
[16] E. Moustafa, S. Mohammed, S. Abdel-Wanis, T. Mahmoud, and E.-S. El-Kady, "Review multi pass friction stir processing," American Scientific Research Journal for Engineering, Technology, and Sciences (ASRJETS), vol. 22, pp. 98-108, 2016.
[17] R. Yamanoğlu, E. Karakulak, A. Zeren, and M. Zeren, "Effect of heat treatment on the tribological properties of Al–Cu–Mg/nanoSiC composites," Materials & Design, vol. 49, pp. 820-825, 2013.
[18] K. Elangovan and V. Balasubramanian, "Influences of post-weld heat treatment on tensile properties of friction stir-welded AA6061 aluminum alloy joints," Materials characterization, vol. 59, pp. 1168-1177, 2008.

[19] X. Ju, F. Zhang, Z. Chen, G. Ji, M. Wang, Y. Wu, et al., "Microstructure of Multi-Pass Friction-Stir-Processed Al-Zn-Mg-Cu Alloys Reinforced by Nano-Sized TiB_2 Particles and the Effect of T6 Heat Treatment," Metals, vol. 7, p. 530, 2017.
[20] E. B. Moustafa, S. Mohammed, S. Abdel-Wanis, M. Abd-Elwahed, T. Mahmoud, and E.-S. El-Kady, "Taguchi optimization for AA2024/Al_2O_3 surface composite hardness fabricating by Friction stir processing," International Research Journal of Engg. and Technol, vol. 3, pp. 7-10, 2016.
[21] Y. Birol, "Precipitation during homogenization cooling in AlMgSi alloys," Transactions of Nonferrous Metals Society of China, vol. 23, pp. 1875-1881, 2013.
[22] W. Yang, S. Ji, L. Huang, X. Sheng, Z. Li, and M. Wang, "Initial precipitation and hardening mechanism during non-isothermal aging in an Al–Mg–Si–Cu 6005A alloy," Materials Characterization, vol. 94, pp. 170-177, 2014.
[23] G. Mrówka-Nowotnik and J. Sieniawski, "Influence of heat treatment on the microstructure and mechanical properties of 6005 and 6082 aluminium alloys," Journal of Materials Processing Technology, vol. 162, pp. 367-372, 2005.
[24] A. Kurt, I. Uygur, and E. Cete, "Surface modification of aluminium by friction stir processing," Journal of materials processing technology, vol. 211, pp. 313-317, 2011.
[25] R. S. Mishra, Z. Ma, and I. Charit, "Friction stir processing: a novel technique for fabrication of surface composite," Materials Science and Engineering: A, vol. 341, pp. 307-310, 2003.
[26] Z. Ma, "Friction stir processing technology: a review," Metallurgical and Materials Transactions A, vol. 39, pp. 642-658, 2008.
[27] T. McNelley, S. Swaminathan, and J. Su, "Recrystallization mechanisms during friction stir welding/processing of aluminum alloys," Scripta Materialia, vol. 58, pp. 349-354, 2008.
[28] T. Prakash, S. Sivasankaran, and P. Sasikumar, "Mechanical and Tribological Behaviour of Friction-Stir-Processed Al 6061 Aluminium Sheet Metal Reinforced with Al_2O_3/0.5Gr Hybrid Surface Nanocomposite," Arab J Sci Eng, vol. 40, pp. 559–569, 2014.
[29] M. S. El-Deeb, S. Khodir, S. A. Abdallah, and A. G. T. Mahmoud, "Effect of Friction Stir Welding Process Parameters and Post-Weld Heat Treatment on the Microstructure and Mechanical Properties of AA6061-O Aluminum Alloys," Journal of American Science, vol. 12, 2016.
[30] D. Aruri, K. Adepu, K. Adepu, and K. Bazavada, "Wear and mechanical properties of 6061-T6 aluminum alloy surface hybrid composites [(SiC+ Gr) and (SiC+ Al_2O_3)] fabricated by friction stir processing," journal of materials research and technology, vol. 2, pp. 362-369, 2013.